Dyes and Pigments 227 (2024) 112178

Contents lists available at ScienceDirect

Dyes and Pigments

journal homepage: www.elsevier.com/locate/dyepig

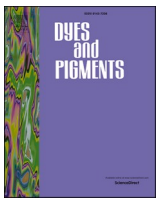

Sulfur-substituted perylenediimides: Easy tunability of the electronic character

Nathalie Zink-Lorre [a], Enrique Font-Sanchis [a], Emilio San-Fabián [b], Fernando Fernández-Lázaro [a,*]

[a] Área de Química Orgánica, Instituto de Bioingeniería, Universidad Miguel Hernández de Elche, Elche, 03202, Spain
[b] Departamento de Química Física and IUMA, Universidad de Alicante, Alicante, 03080, Spain

A B S T R A C T

Perylenediimides (PDIs) are the focus of a huge number of research lines for their awesome properties which can be modulated over a wide range by chemical modification of their structure. However, industrial applications require reduced costs in materials preparation and transformation. In this contribution we explore the ability of sulfur-substituted PDIs to vary their electronic character from strong electron-donating to strong electron-accepting in just one reaction.

1. Introduction

Perylenediimides (PDIs) are functional materials involved in the field of organic electronics which have been extensively studied due to their high electron affinities and charge carrier mobilities [1]. Thus, among high performance n-type materials, the PDIs hold the distinction of having one of the highest n-type mobilities known [2]. Furthermore, they are also well-known for their intense red or orange colors, their fluorescence quantum yields close to the unity and their thermal, chemical, and photochemical stabilities [3]. In addition to the outstanding electrical properties, PDI-based materials have demonstrated great promise due to their ability to yield air-stable semiconducting films from solution [4]. As a result of all of this, they have been very attractive for the development of n-type semiconducting materials [5], artificial photosynthetic systems [6], solar cells [7], biolabels [8], lasers [9] or sensors [10].

On the other hand, chemical functionalization of PDIs *via* core substitution results in the possibility to modify the properties of PDIs in an extraordinary wide range. Thus, it is possible to vary their color from the typical red (e.g. core-unsubstituted PDI, λ_{max} = 525 nm) to deep blue (1,6,7-tripiperidin-*N*′-ylPDI, λ_{max} = 706 nm) passing through the complete rainbow [11]. It is also possible to turn the well-known strong electron-accepting character of PDIs (1,7-dicianoPDI, $E_{red} = -0.07$ V *vs.* Fc/Fc^{+}) [12] into a strong electron-donor one (1,6,7-tripiperidin-*N*′-ylPDI, $E_{ox} = 0.06$ V *vs.* Fc/Fc^{+}) [11]. In particular, it is feasible to lower the energy of the lowest unoccupied molecular orbital (LUMO), in order to obtain compounds with an enhanced stability and accessible for the efficient injection of charge carriers [4,13]. Thus, LUMO values as low as −4.75 eV for 1,6,7,12-tetraphenylsulfonylPDI have been described [14].

However, this modulation capacity of the properties requires the preparation of molecules with quite different substituents which could be a drawback for the industrial application as it will require diverse synthetic pathways. Thus, it would be desirable to have substituents delivering very different properties to the PDI but with a synthetic pathway as close as possible. In this sense, the purpose of this work is to demonstrate the possibility to modulate the electron donor/accepting character of the PDIs by controlling the oxidation state of the sulfur atoms in S-substituted PDIs. To this end, we have compared the optical and electrochemical behavior of alkylsulfide-, alkylsulfinyl- and alkylsulfonylPDIs for all the usual PDI substitution patterns, namely 1-monosubstituted, 1,6-disubstituted, 1,7-disubstituted, 1,6,7,12-tetrasubstituted (bay-tetrasubstituted) and 2,5,8,11-tetrasubstituted (*ortho*-tetrasubstituted). It must be mentioned here that there are a few similar studies, although more limited in scope. Thus, the properties of a tetra(alkylthio)terrylenediimide and its corresponding tetrasulfonyl derivative have been described [15]. Analogously, there is a communication comparing two alkylthio bay-tetrasubstituted PDIs with the sulfones derived from them [14].

* Corresponding author.
E-mail address: fdofdez@umh.es (F. Fernández-Lázaro).

https://doi.org/10.1016/j.dyepig.2024.112178
Received 27 July 2023; Received in revised form 10 April 2024; Accepted 22 April 2024
Available online 23 April 2024
0143-7208/© 2024 The Authors. Published by Elsevier Ltd. This is an open access article under the CC BY-NC-ND license (http://creativecommons.org/licenses/by-nc-nd/4.0/).

2. Experimental

2.1. Chemicals, instruments and theoretical calculations

Solvents and reagents were obtained from commercial sources and used as received. Column chromatography: SiO_2 (40–63 μm). TLC plates coated with SiO_2 60F254 were visualized by UV light. NMR spectra were recorded at 25 °C using a Bruker AC300 spectrometer. The solvents for spectroscopic studies were of spectroscopic grade and used as received. UV vis spectra were measured with a Helios Gamma spectrophotometer. Fluorescence emission spectra were recorded on a PerkinElmer LS55 spectrofluorometer and fluorescence quantum yields were calculated using PDI **1** as the standard ($\Phi_f = 1$)[1a] and following the procedure described elsewhere [16]. IR spectra were recorded with a Nicolet Impact 400D spectrophotometer. High resolution Mass spectra were obtained from a Bruker Reflex II matrix-assisted laser desorption/ionization time of flight (MALDI-TOF) using dithranol as matrix. Cyclic and differential pulse voltammetry measurements were performed at 298 K in a conventional three-electrode cell using a *m*-AUTOLAB type III potentiostat/galvanostat. Sample solutions were prepared in dichloromethane, containing 0.10 M tetrabutylammonium hexafluorophosphate ($TBAPF_6$) as supporting electrolyte. A glassy carbon (GC) working electrode, an $Ag/AgNO_3$ reference electrode, and a platinum wire counter electrode were used. Ferrocene/ferrocenium was the internal standard for all measurements.

Density functional theory (DFT) calculations were performed by using Gaussian 16, Revision C.01 [17]. Minimum-energy geometry was obtained using the hybrid Becke3–Lee–Yang–Parr (B3LYP) [18] functional and the Pople's double-zeta 6-31G* basis set [19]. Frequency calculations were performed to confirm the minimum nature of the structure. Molecular orbitals were represented using Avogadro: an open-source molecular builder and visualization tool. Version 1.2.0 [20]. Calculations on the excited states were performed with the hybrid meta GGA functional M06-2X [21].

2.2. Preparation of perylenediimide derivatives *1*–*10*

PDIs **1** [1a], **4** [22], **6** [23], **8** [24] and **9** [25] were synthesized following the procedures described elsewhere.

2.2.1. *N,N′-di(hexylheptyl)-1-butylthioperylene-3,4:9,10-tetracarboxydiimide (2)*

A mixture of 36 mg (0.4 mmol) of butanethiol, 14 mg (0.24 mmol) of KF and 126 mg (0.48 mmol) of 18-crown-6 was added to a solution of 75 mg (0.1 mmol) of *N,N′*-di(hexylheptyl)perylene-3,4:9,10-tetracarboxydiimide in dry THF (0.3 mL). The reaction was refluxed 24 h under argon atmosphere and, after cooling, it was extracted with dichloromethane and washed with water. The organic layer was dried over anhydrous sodium sulfate, filtered and evaporated. Purification was carried out by silica gel column chromatography using toluene as eluent yielding 40 mg of **2** as a violet powder.

Yield: 47 %. ^{1}H NMR ($CDCl_3$) δ 0.83 (t, 12H), 0.94 (t, 3H), 1.25 (br, 32H), 1.49 (m, 2H), 1.70 (m, 2H), 1.87 (m, 4H), 2.27 (m, 4H), 3.27 (t, 2H), 5.20 (m, 2H), 8.64 (d, 3H), 8.74 (br, 3H), 8.97 (d, 1H). ^{13}C NMR ($CDCl_3$) δ 164.71, 163.54, 139.83, 139.24, 134.22, 133.98, 133.37, 132.72, 131.20, 130.44, 129.19, 128.92, 127.79, 127.07, 126.50, 123.49, 122.36, 114.04, 54.66, 35.87, 33.80, 32.38, 31.90, 31.75, 31.74, 31.41, 30.45, 29.67, 29.63, 29.34, 29.21, 29.19, 29.13, 28.93, 26.91, 22.57, 22.56, 22.03, 14.01, 13.59. MS MALDI-TOF *m/z*: [M^+] calcd. for $C_{54}H_{70}N_2O_4S$: 842.5050, found: 842.5104. IR (KBr): 2961, 2926, 2851, 1707, 1654, 1579, 1386, 1323, 1240, 803, 756 cm^{-1}. UV–vis (CH_2Cl_2), λ_{max}/nm (log ε): 444 (4.2), 542 (4.57).

2.2.2. *N,N′-di(hexylheptyl)-1,6-di(butylthio)perylene-3,4:9,10-tetracarboxydiimide (3)*

A mixture of 126 mg (1.4 mmol) of butanethiol, 21 mg (0.36 mmol) of KF and 190 mg (0.72 mmol) of 18-crown-6 was added to a solution of 75 mg (0.1 mmol) of *N,N′*-di(hexylheptyl)perylene-3,4:9,10-tetracarboxydiimide in dry THF (2 mL). The reaction was refluxed 24 h under argon atmosphere and, after cooling, it was extracted with dichloromethane and washed with water. The organic layer was dried over anhydrous sodium sulfate, filtered and evaporated. Purification was carried out by silica gel column chromatography using toluene as eluent yielding 40 mg of **3** as a violet powder.

Yield: 43 % (pure 1,6-isomer). ^{1}H NMR ($CDCl_3$) δ 0.83 (t, 12H), 0.92 (t, 6H), 1.25 (br, 32H), 1.46 (m, 4H), 1.68 (m, 4H), 1.87 (m, 4H), 2.28 (m, 4H), 3.23 (t, 4H), 5.20 (m, 2H), 8.67 (br, 2H), 8.76 (br, 2H), 8.86 (d, 2H). ^{13}C NMR ($CDCl_3$) δ 164.62, 163.57, 138.54, 132.65, 132.37, 131.32, 130.57, 129.40, 128.90, 128.47, 128.04, 127.87, 125.63, 114.04, 54.79, 35.62, 32.42, 31.75, 31.74, 30.48, 29.67, 29.21, 26.91, 22.58, 22.57, 22.01, 14.02, 13.58. MS MALDI-TOF *m/z*: [M^+] calcd. for $C_{58}H_{78}N_2O_4S_2$: 930.5397, found 930.5072. IR (KBr): 2956, 2921, 2851, 1707, 1654, 1584, 1468, 1404, 1345, 803, 738 cm^{-1}. UV–vis (CH_2Cl_2), λ_{max}/nm (log ε): 428 (4.2), 565 (4.5).

2.2.3. *N,N′-di(hexylheptyl)-1,7-di(butylthio)perylene-3,4:9,10-tetracarboxydiimide (5)*

A mixture of 36 mg (0.4 mmol) of butanethiol, 29 mg (0.5 mmol) of KF and 266 mg (1 mmol) of 18-crown-6 was added to a solution of 100 mg (0.1 mmol) of *N,N′*-di(hexylheptyl)-1,7(6)-dibromoperylene-3,4:9,10-tetracarboxydiimide in dry THF (2 mL). The reaction was refluxed 24 h under argon atmosphere and, after cooling, it was extracted with dichloromethane and washed with water. The organic layer was dried over anhydrous sodium sulfate, filtered and evaporated. Purification was carried out by silica gel column chromatography using dichloromethane:hexane 1:1 as eluent yielding 64 mg of **5** as a violet powder.

Yield: 70 % (pure 1,7-isomer). ^{1}H NMR ($CDCl_3$) δ 0.83 (t, 12H), 0.91 (t, 6H), 1.23 (br, 32H), 1.48 (m, 4H), 1.68 (m, 4H), 1.86 (m, 4H), 2.26 (m, 4H), 3.22 (t, 4H), 5.20 (m, 2H), 8.65–8.84 (br, 6H). ^{13}C NMR ($CDCl_3$) δ 164.59, 163.63, 139.88, 133.16, 132.63, 132.31, 131.32, 130.54, 129.35, 128.94, 128.87, 128.63, 128.44, 128.27, 128.02, 127.85, 125.60, 122.62, 122.13, 121.87, 121.44, 54.89, 54.73, 54.61, 35.77, 35.60, 32.40, 31.74, 30.88, 30.46, 29.20, 26.90, 22.55, 22.03, 21.99, 14.01, 13.57, 13.56. MS MALDI-TOF *m/z*: [M^+] calcd. for $C_{58}H_{78}N_2O_4S_2$: 930.5397, found: 930.5065. IR (KBr): 2961, 2921, 2851, 1701, 1649, 1590, 1462, 1404, 1316, 1234, 1094, 808 cm^{-1}. UV–vis (CH_2Cl_2), λ_{max}/nm (log ε): 428 (4.1), 565 (4.5).

2.2.4. *N,N′-di(hexylheptyl)-1,6,7,12-tetra(butylthio)perylene-3,4:9,10-tetracarboxydiimide (7)*

A mixture of 108 mg (1.2 mmol) of butanethiol, 76 mg (1.2 mmol) of KF and 640 mg (2.4 mmol) of 18-crown-6 was added to a solution of 106 mg (0.12 mmol) of *N,N′*-di(hexylheptyl)-1,6,7,12-tetrachloroperylene-3,4:9,10-tetracarboxydiimide in dry THF (2 mL). The reaction was refluxed 12 h under argon atmosphere and, after cooling, it was extracted with dichloromethane and washed with water. The organic layer was dried over anhydrous sodium sulfate, filtered and evaporated. Purification was carried out by silica gel column chromatography using dichloromethane:hexane 1:1 as eluent yielding 132 mg of **7** as a violet powder.

Yield: 99 %. ^{1}H NMR ($CDCl_3$) δ 0.75 (t, 12H), 0.84 (t, 12H), 1.25 (br, 32H), 1.46 (m, 8H), 1.87 (m, 4H), 2.25 (m, 4H), 2.96 (m, 8H), 5.20 (m, 2H), 8.67 (d, 4H). ^{13}C NMR ($CDCl_3$) δ 164.83, 163.73, 139.42, 131.86, 131.02, 129.28, 122.88, 121.75, 121.04, 54.80, 36.31, 32.51, 32.47, 31.76, 30.79, 29.69, 29.25, 29.24, 26.98, 26.95, 22.59, 21.93, 14.03, 13.50. MS MALDI-TOF *m/z*: [M^+] calcd. for $C_{66}H_{94}N_2O_4S_4$: 1106.6096, found: 1106.6728. IR (KBr): 2961, 2944, 2856, 1695, 1654, 1579, 1380, 1275, 1240, 820, 744 cm^{-1}. UV–vis (CH_2Cl_2), λ_{max}/nm (log ε): 565 (4.4).

2.2.5. N,N′-di(hexylheptyl)-2,5,8,11-tetra(butylthio)perylene-3,4:9,10-tetracarboxydiimide (10)

A mixture of 54 mg (0.6 mmol) of butanethiol, 38 mg (0.6 mmol) of KF and 316 mg (1.2 mmol) of 18-crown-6 was added to a solution of 70 mg (0.06 mmol) of *N,N′*-di(hexylheptyl)-2,5,8,11-tetrabromoperylene-3,4:9,10-tetracarboxydiimide in dry THF (2 mL). The reaction was refluxed 24 h under argon atmosphere and, after cooling, it was extracted with dichloromethane and washed with water. The organic layer was dried over anhydrous sodium sulfate, filtered and evaporated. Purification was carried out by silica gel column chromatography using dichloromethane:hexane 1:1 as eluent yielding 50 mg of **10** as an orange powder.

Yield: 76 %. ^{1}H NMR ($CDCl_3$) δ 0.83 (t, 12H), 1.05 (t, 12H), 1.26 (br, 32H), 1.66 (m, 8H), 1.91 (m, 12H), 2.24 (m, 4H), 3.20 (t, 8H), 5.23 (m, 2H), 8.38 (s, 4H). ^{13}C NMR ($CDCl_3$) δ 163.83, 163.29, 150.52, 131.80, 120.03, 117.83, 116.36, 54.83, 32.28, 32.10, 31.65, 29.79, 29.56, 29.13, 27.04, 22.53, 22.47, 13.94, 13.74. MS MALDI-TOF *m/z*: [M^+] calcd. for $C_{66}H_{94}N_2O_4S_4$: 1106.6096, found: 1106.6970. IR (KBr): 2921, 2851, 1684, 1637, 1590, 1561, 1520, 1462, 1351, 1246 cm^{-1}. UV–vis (CH_2Cl_2), λ_{max}/nm (log ε): 380 (3.9), 400 (4.0), 488 (4.7), 543 (4.7).

2.3. Sulfur oxidation of PDI derivatives

2.3.1. Synthesis of N,N′-di(hexylheptyl)-1-butylsulfinylperylene-3,4:9,10-tetracarboxydiimide (11)

M-chloroperbenzoic acid (0.2 mmol) was added to a solution of **2** (0.02 mmol) in dichloromethane (1 mL). The mixture was stirred at −78 °C for 5 h and washed with water. The organic layer was dried over anhydrous sodium sulfate, filtered and evaporated. Purification was carried out by silica gel column chromatography using dichloromethane:acetone (8:0.2) as eluent.

Yield: 75 %. ^{1}H NMR ($CDCl_3$) δ 0.83 (t, 12H), 0.97 (t, 3H), 1.23 (br, 32H), 1.46 (m, 2H), 1.87 (m, 4H), 2.04 (m, 2H), 2.26 (m, 4H), 2.94 (m, 1H), 3.08 (m, 1H), 5.19 (m, 2H), 8.27 (d, 1H), 8.72 (br, 5H), 9.52 (s, 1H). ^{13}C NMR ($CDCl_3$) δ 164.26, 163.42, 146.66, 134.74, 133.84, 133.40, 130.39, 129.88, 129.25, 127.62, 126.93, 123.92, 123.57, 55.27, 54.94, 32.33, 31.91, 31.73, 29.68, 29.35, 29.18, 26.89, 25.46, 22.56, 21.79, 14.02, 13.69. MS MALDI-TOF *m/z*: [M^+] calcd. for $C_{54}H_{70}N_2O_5S$: 858.4999, found: 858.4926. IR (KBr): 2932, 2851, 1707, 1660, 1590, 1380, 1334, 1240, 803 cm^{-1}. UV–vis (CH_2Cl_2), λ_{max}/nm (log ε): 502 (4.6), 524 (4.7).

2.3.2. Synthesis of sulfoxides 12 and 13

M-chloroperbenzoic acid (0.3 mmol) was added to a solution of the PDI (0.02 mmol) in dichloromethane (1 mL). The mixture was stirred at −78 °C for 5 h and washed with water. The organic layer was dried over anhydrous sodium sulfate, filtered and evaporated. Purification was carried out by silica gel column chromatography using dichloromethane:acetone (8:0.2) as eluent.

2.3.2.1. N,N′-di(hexylheptyl)-1,6-di(butylsulfinyl)perylene-3,4:9,10-tetracarboxydiimide (12).

Yield: 82 % from **3**. ^{1}H NMR ($CDCl_3$) δ 0.82 (m, 12H), 0.92 (m, 6H), 1.22 (br, 32H), 1.56 (m, 4H), 1.86 (m, 4H), 1.99 (m, 4H), 2.26 (m, 4H), 2.88 (m, 1H), 3.07 (m, 3H), 5.19 (m, 2H), 8.19 (m, 1H), 8.46 (d, 1H), 8.77 (br, 2H), 9.53 (s, 2H). ^{13}C NMR ($CDCl_3$) δ 163.94, 163.44, 162.80, 162.36, 146.92, 146.83, 146.56, 133.06, 132.72, 132.54, 132.42, 131.59, 130.75, 130.37, 129.31, 129.13, 128.43, 128.33, 128.02, 127.63, 124.63, 123.88, 55.64, 55.49, 55.13, 32.27, 31.68, 29.62, 29.12, 26.83, 25.34, 22.51, 21.76, 21.68, 13.97, 13.61. MS MALDI-TOF *m/z*: [M^+] calcd. for $C_{58}H_{78}N_2O_6S_2$: 962.5295, found: 962.5465. IR (KBr): 2956, 2932, 2856, 1695, 1654, 1590, 1474, 1398, 1334, 1246, 1124, 814 cm^{-1}. UV–vis (CH_2Cl_2), λ_{max}/nm (log ε): 509 (4.4).

2.3.2.2. N,N′-di(hexylheptyl)-1,7-di(butylsulfinyl)perylene-3,4:9,10-tetracarboxydiimide (13).

Yield: 98 % from **5**. ^{1}H NMR ($CDCl_3$) δ 0.81 (t, 12H), 0.91 (m, 6H), 1.21 (br, 32H), 1.59 (m, 4H), 1.83 (m, 4H), 1.99 (m, 4H), 2.25 (m, 4H), 2.88 (m, 1H), 3.05 (m, 3H), 5.18 (m, 2H), 8.19 (m, 1H), 8.46 (d, 1H), 8.76 (br, 2H), 9.52 (s, 2H). ^{13}C NMR ($CDCl_3$) δ 163.83, 163.36, 162.77, 162.24, 146.85, 146.75, 146.48, 133.11, 132.98, 132.64, 132.45, 132.33, 131.79, 131.76, 131.39, 130.66, 130.29, 129.73, 129.22, 129.05, 128.37, 128.35, 128.25, 127.94, 127.55, 126.99, 124.35, 123.74, 55.55, 55.41, 55.04, 32.18, 32.13, 31.60, 29.03, 26.74, 25.25, 22.42, 21.67, 21.60, 13.89, 13.55, 13.54, 13.53. MS MALDI-TOF *m/z*: [M + H^+] calcd. for $C_{58}H_{78}N_2O_6S_2$: 963.5295 found: 963.5721. IR (KBr): 2961, 2915, 2856, 1701, 1666, 1579, 1468, 1380, 1322, 1240 cm^{-1}. UV–vis (CH_2Cl_2), λ_{max}/nm (log ε): 526 (4.8).

2.3.3. Synthesis of sulfones 14-16

M-chloroperbenzoic acid (0.4 mmol) was added to a solution of the PDI (0.02 mmol) in dichloromethane (1 mL). The mixture was stirred at room temperature for 6 h and washed with water. The organic layer was dried over anhydrous sodium sulfate, filtered and evaporated. Purification was carried out by silica gel column chromatography using dichloromethane:acetone (8:0.2) as eluent.

2.3.3.1. N,N′-di(hexylheptyl)-1-butylsulfonylperylene-3,4:9,10-tetracarboxydiimide (14).

Yield: 92 % from **2**. ^{1}H NMR ($CDCl_3$) δ 0.82 (t, 16H), 1.22 (br, 34H), 1.65 (m, 2H), 1.87 (m, 4H), 2.26 (m, 4H), 3.37 (t, 2H), 5.18 (m, 2H), 8.70 (br, 5H), 9.20 (br, 2H). ^{13}C NMR ($CDCl_3$) δ 164.17, 163.41, 138.62, 136.44, 135.37, 134.93, 133.27, 132.72, 131.40, 131.09, 130.73, 130.14, 129.76, 128.35, 128.05, 126.30, 124.06, 123.94, 123.02, 122.42, 55.09, 54.87, 54.52, 32.32, 32.24, 31.68, 29.14, 29.11, 26.85, 24.31, 22.51, 21.37, 13.97, 13.29. MS MALDI-TOF *m/z*: [M^+] calcd. for $C_{54}H_{70}N_2O_6S$: 874.4949, found: 874.4796. IR (KBr): 2956, 2932, 2856, 1695, 1654, 1590, 1474, 1398, 1334, 1246, 1124, 814 cm^{-1}. UV–vis (CH_2Cl_2), λ_{max}/nm (log ε): 494 (4.6), 528 (4.72).

2.3.3.2. N,N′-di(hexylheptyl)-1,6-di(butylsulfonyl)perylene-3,4:9,10-tetracarboxydiimide (15).

Yield: 87 % from **3**. ^{1}H NMR ($CDCl_3$) δ 0.84 (m, 18H), 1.24 (br, 36H), 1.63 (m, 4H), 1.87 (m, 4H), 2.21 (m, 4H), 3.48 (t, 4H), 5.19 (m, 2H), 8.81 (s, 2H), 9.00 (d, 2H), 9.18 (s, 2H). ^{13}C NMR ($CDCl_3$) δ 163.54, 162.32, 139.02, 135.78, 134.28, 131.39, 130.20, 129.48, 128.37, 127.93, 55.10, 31.71, 29.14, 26.86, 22.54, 21.48, 14.00, 13.38. MS MALDI-TOF *m/z*: [M^+] calcd. for $C_{58}H_{78}N_2O_8S_2$: 994.5194, found: 994.5306. IR (KBr): 2950, 2925, 2856, 1704, 1659, 1589, 1458, 1401, 1328, 1234, 1127, 805 cm^{-1}. UV–vis (CH_2Cl_2), λ_{max}/nm (log ε): 492 (4.4), 526 (4.5).

2.3.3.3. N,N′-di(hexylheptyl)-1,7-di(butylsulfonyl)perylene-3,4:9,10-tetracarboxydiimide (16).

Yield: 92 % from **5**. ^{1}H NMR ($CDCl_3$) δ 0.84 (m, 18H), 1.23 (br, 36H), 1.70 (m, 4H), 1.86 (m, 4H), 2.21 (m, 4H), 3.27 (t, 1H), 3.48 (t, 3H), 5.18 (m, 2H), 8.81 (br, 2H), 9.02 (d, 2H), 9.27 (m, 2H). ^{13}C NMR ($CDCl_3$) δ 163.54, 162.41, 139.62, 139.02, 135.78, 134.89, 134.63, 134.26, 133.61, 131.39, 130.88, 130.16, 129.78, 128.81, 128.38, 128.21, 127.93, 55.10, 32.30, 31.71, 29.67, 29.14, 26.86, 24.35, 22.54, 21.48, 14.00, 13.38. MS MALDI-TOF *m/z*: [M^+] calcd. for $C_{58}H_{78}N_2O_8S_2$: 994.5194, found: 994.5424. IR (KBr): 2915, 2839, 1701, 1660, 1590, 1462, 1398, 1328, 1234, 1124 cm^{-1}. UV–vis (CH_2Cl_2), λ_{max}/nm (log ε): 490 (4.3), 525 (4.5).

2.3.4. Synthesis of sulfones 17-19

M-chloroperbenzoic acid (0.5 mmol) was added to a solution of the PDI (0.02 mmol) in dichloromethane (1 mL). The mixture was stirred at room temperature for 8 h and washed with water. The organic layer was dried over anhydrous sodium sulfate, filtered and evaporated. Purification was carried out by silica gel column chromatography using dichloromethane:acetone (8:0.2) as eluent.

2.3.4.1. N,N′-di(hexylheptyl)-1,6,7,12-tetra(butylsulfonyl)perylene-3,4:9,10-tetracarboxydiimide (17). Yield: 86 % from **7**. ^{1}H NMR ($CDCl_3$) δ 0.84 (t, 24H), 1.25 (br, 40H), 1.69 (m, 4H), 1.83 (m, 8H), 1.87 (m, 4H), 3.07 (m, 4H), 3.55 (m, 4H), 5.18 (m, 2H), 9.08 (s, 1H). ^{13}C NMR ($CDCl_3$) δ 162.70, 161.44, 145.72, 130.55, 129.87, 129.18, 127.95, 127.15, 124.72, 124.03, 56.48, 55.79, 32.42, 32.26, 31.71, 31.68, 29.67, 29.21, 29.18, 26.95, 26.92, 23.33, 22.59, 21.57, 14.01, 13.48. MS MALDI-TOF *m/z*: [M^+] calcd. for $C_{66}H_{94}N_2O_{12}S_4$: 1234.684, found: 1234.5524. IR (KBr): 2966, 2921, 2852, 1708, 1667, 1589, 1467, 1409, 1377, 1328, 1262, 1131, 1095, 1028, 809 cm^{-1}. UV–vis (CH_2Cl_2), λ_{max}/nm (log ε): 497 (4.3), 531 (4.4).

2.3.4.2. N,N′-di(hexylheptyl)-2,5,8,11-tetra(butylsulfonyl)perylene-3,4:9,10-tetracarboxydiimide (18). Yield: 90 % from **10**. ^{1}H NMR ($CDCl_3$) δ 0.84 (t, 12H), 0.99 (t, 12H), 1.25 (br, 32H), 1.55 (m, 8H), 1.82 (m, 4H), 1.95 (m, 8H), 2.24 (m, 4H), 4.04 (t, 8H), 5.07 (m, 2H), 9.47 (s, 4H). ^{13}C NMR ($CDCl_3$) δ 161.66, 145.72, 132.77, 129.73, 129.14, 127.86, 126.49, 56.78, 32.26, 31.66, 29.08, 26.68, 24.46, 22.57, 21.70, 14.02, 13.55. MS MALDI-TOF *m/z*: [M^+] calcd. for $C_{66}H_{94}N_2O_4S_4$: 1234.5684, found: 1234.5016. IR (KBr): 2967, 2938, 2862, 1713, 1666, 1590, 1555, 1433, 1316, 1129, 715, 575 cm^{-1}. UV–vis (CH_2Cl_2), λ_{max}/nm (log ε): 468 (4.2), 499 (4.6), 537 (4.9).

2.3.4.3. N,N′-di(hexylheptyl)-2,3,10,11-tetrahydroperyleno[6,6a,6b,7-efg:12,12a,12b,1-e′f′g′]bis([1,4]dithiocine)1,1,4,4,9,9,12,12-octaoxide-6,7:14,15-tetracarboxydiimide (19). Yield: 80 % from **8**. ^{1}H NMR ($CDCl_3$) δ 0.80 (m, 12H), 1.20 (br, 32H), 1.83 (m, 4H), 2.21 (m, 4H), 4.00 (d, 4H), 4.22 (d, 4H), 5.16 (m, 2H), 9.28 (s, 4H). ^{13}C NMR ($CDCl_3$) δ 162.67, 161.39, 143.42, 142.50, 133.65, 133.02, 130.63, 129.49, 127.94, 125.32, 123.76, 55.99, 50.72, 32.39, 32.23, 31.68, 31.64, 31.61, 29.16, 26.87, 22.57, 22.56, 14.00, 13.99, 13.97. MS MALDI-TOF *m/z*: [M^+] calcd. for $C_{74}H_{110}N_2O_{12}S_4$: 1062.3493, found: 1062.3631. IR (KBr) 2921, 2860, 1720, 1663, 1593, 1381, 1336, 1283, 1164, 1140, 1115, 735 cm^{-1}. UV–vis (CH_2Cl_2), λ_{max}/nm (log ε): 492 (4.4), 527 (4.6).

3. Results and discussion

3.1. Synthesis of perylene dyes

PDIs **2**, **3**, **5**, **7**, **8** and **10** have been synthesized following a fluoride-mediated general procedure described previously by us (Scheme 1) [24, 26]. We selected *N,N′*-di(hexylheptyl)perylenediimide **1**, *N,N′*-di(hexylheptyl)-1,7(6)-dibromoperylenediimide **4**, *N,N′*-di(hexylheptyl)-1,6,7,12-tetrachloroperylenediimide **6** and *N,N′*-di(hexylheptyl)-2,5,8,11-tetrabromoperylenediimide **9** as starting materials for our study due to their high solubility in most organic solvents and being aware that the substituents at the imide nitrogen do not alter the electronic structure of the PDI [1]. Butanethiol was selected as reagent due to its moderately high boiling point. The aliphatic thiol reacts with the appropriated halogenated PDIs in the presence of fluoride anions affording PDIs **5**, **7** and **10** with yields ranging from 70 to 99 %. On the other hand, reaction with the naked PDI **1** affords mixtures of PDIs **2** and **3**, but adjusting the reactant ratios in different reactions it was possible to obtain these compounds in 47 and 43 % yield, respectively. In this way, it was possible to obtain a family of PDIs functionalized following different patterns that cover all positions of the aromatic core.

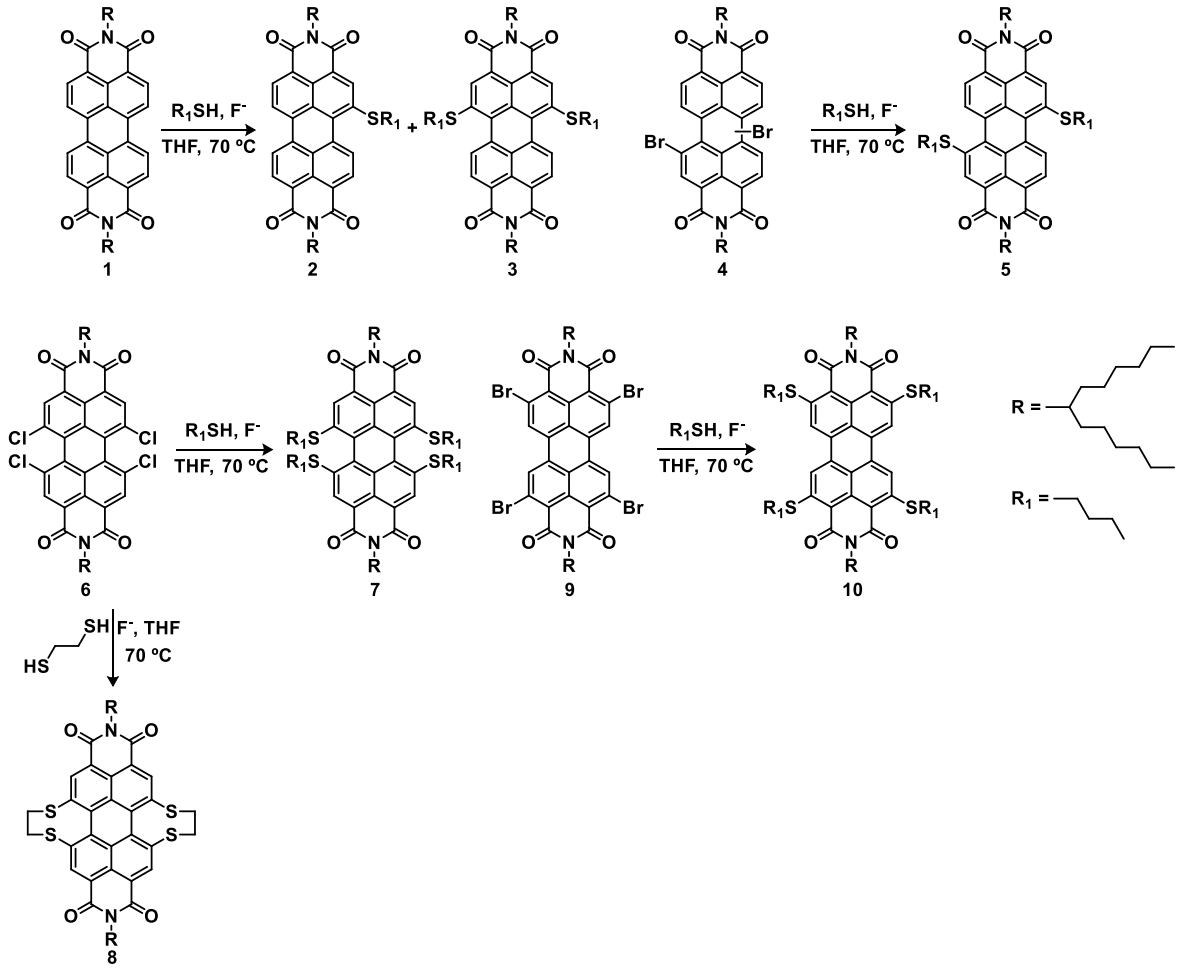

Scheme 1. Synthesis of PDIs **2**, **3**, **5**, **7**, **8**, and **10**.

Then, we faced the synthesis of the sulfinyl and sulfonyl derivatives **11**–**19** using *m*-chloroperbenzoic acid (*m*-CPBA) as an oxidizing agent (Chart 1). The preparation of either sulfinyl or sulfonyl derivatives could be controlled by adjusting the amount of *m*-CPBA and the temperature of the reaction. At −78 °C we obtained PDIs **11**–**13** in 75, 82 and 98 % yields, respectively. However, in our hands, the synthesis of the sulfoxides derived from **7**, **8** and **10** was not possible, as we were unable to control the monooxidation of the four thioether groups at the same time. We obtained complex mixtures instead.

On the other hand, derivatives **14**–**19** were obtained with good yields, comprised between 80 and 90 %, at room temperature.

At the end we obtained a large family of PDI derivatives which included mono-, di-, and tetrafunctionalized compounds with a broad substitution pattern (1; 1,6; 1,7; 1,6,7,12 and 2,5,8,11), thus allowing a systematic study of their properties.

The structure of all the compounds was confirmed by ^{1}H NMR, ^{13}C NMR, UV–vis, IR and MALDI-TOF MS (see Figs. S1–S70, ESI).

3.2. Optical characterization

All the synthesized compounds show strong optical absorption in the visible region of the electromagnetic spectrum, an expected characteristic of PDI materials (Table 1). The sulfides show purple color when in solution due to the electron donating character of the sulfur atoms, while the sulfoxides and sulfones originate orange solutions typical of the PDIs with electron accepting substituents.

Fig. 1 compares the UV–vis spectra of all the thioether-substituted PDI derivatives (**2**, **3**, **5**, **7**, **8**, and **10**) to the naked one (**1**) in methylene chloride solution. The spectrum of **1** in solution displays a strong band for the 0–0 transition at 524 nm, and subsequently weaker bands at 488 and 458 nm corresponding to the 0–1 and 0–2 vibronic transitions, respectively.

Table 1
UV–vis absorption (λ_{max}) and fluorescence maximum (λ_{em}) wavelengths, extinction coefficients (log ε), fluorescence quantum yields (Φ), wavelengths of the 0-0 transition ($\lambda_{0\text{-}0}$), and Stokes shifts.

	λ_{max}/nm (log ε), CH_2Cl_2	λ_{em}/nm (Φ), CH_2Cl_2	$\lambda_{0\text{-}0}$/nm	Stokes shift/nm
1	458 (4.6), 488 (5.0), 524 (5.2)	532 (1)	528	8
2	444 (4.2), 542 (4.6)	625 (0.049)	580	83
3	429 (4.2), 566 (4.5)	641 (0.027)	605	76
5	428 (4.1), 444 (4.1) 565 (4.5)	638 (0.03)	605	73
7	579 (4.4)	673 (0.007)	637	94
8	303 (4.5), 402 (3.9), 590 (4.2)	649 (0.003)	622	59
10	380 (3.9), 400 (4.0), 488 (4.7), 543 (4.7)	557 (0.001)	548	14
11	502 (4.6), 524 (4.7)	569 (0.02)	545	45
12	509 (4.4)	559 (0.05)	542	50
13	526 (4.8)	569 (0.02)	553	43
14	494 (4.6), 528 (4.7)	550 (0.54)	540	22
15	492 (4.4), 526 (4.5)	542 (0.52)	535	16
16	490 (4.3), 525 (4.5)	542 (0.53)	534	17
17	497 (4.3), 531 (4.4)	557 (0.44)	544	26
18	468 (4.2), 499 (4.6), 537 (4.9)	551 (0.7)	543	14
19	492 (4.4), 527 (4.6)	545 (0.46)	537	18

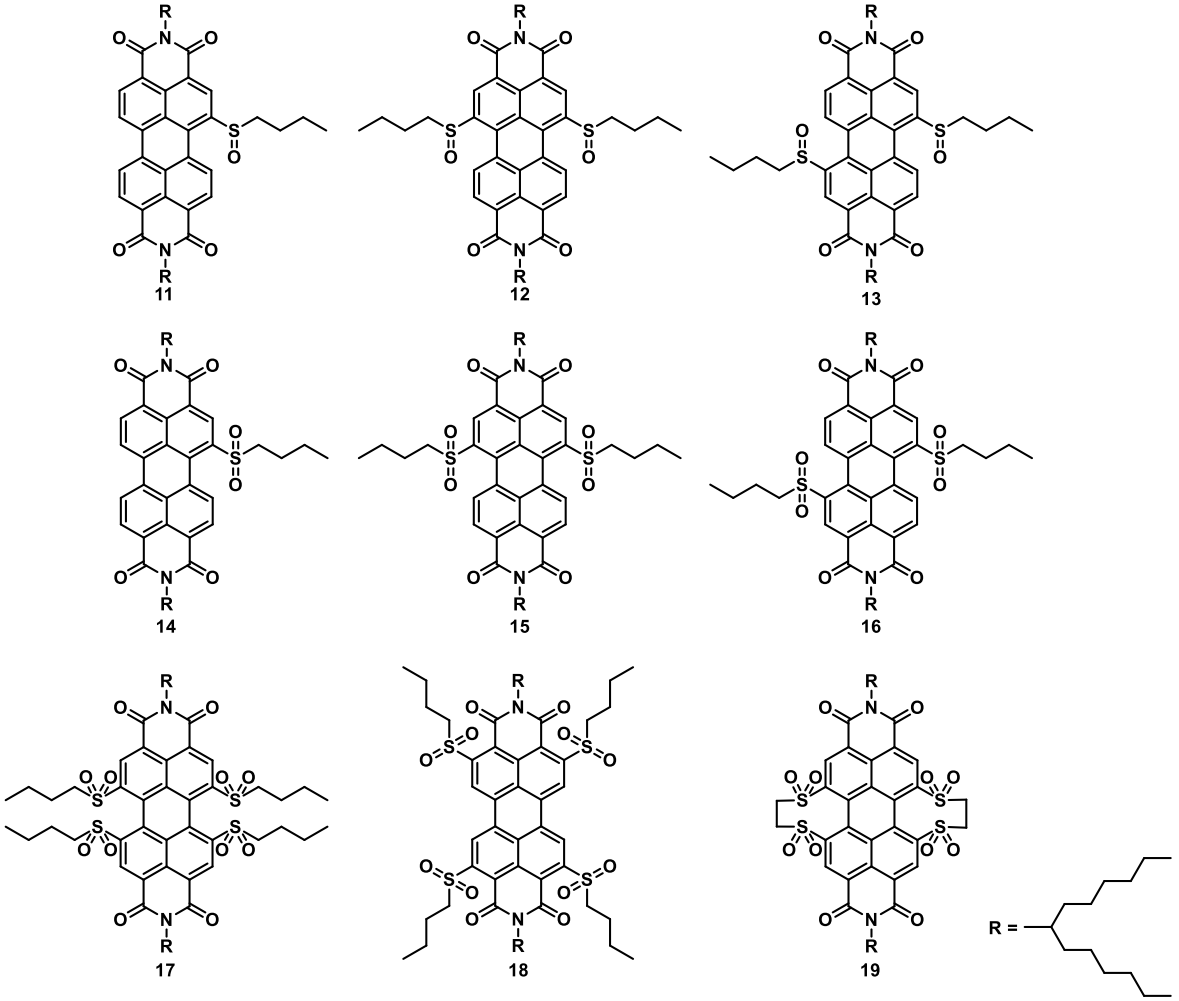

Chart 1. Sulfoxides **11**–**13** and sulfones **14**–**19**.

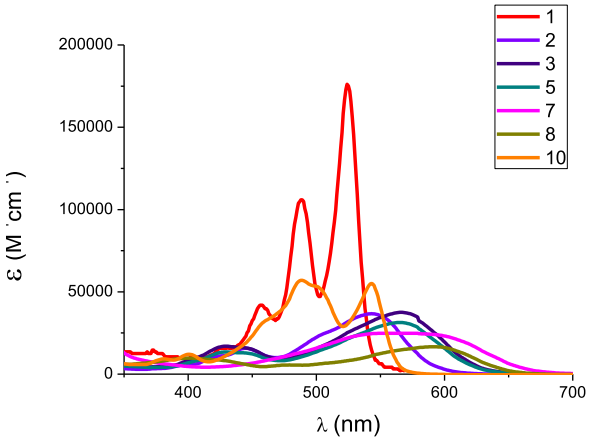

Fig. 1. Absorption spectra of PDIs **1**, **2**, **3**, **5**, **7**, **8** and **10** in CH_2Cl_2 solution.

The introduction of substituents at the bay positions induces a bathochromic shift, more pronounced as the number of substituents increases (Table 1). Thus, the absorption maximum moves to 542 nm for the 1-substituted PDI **2** (18 nm shift respect to PDI **1**), and ca. 565 nm for the 1,6- and 1,7-disubstituted PDIs **3** and **5** (41 nm shift respect to PDI **1**). The highest shifts correspond to the bay tetrasubstituted PDIs **7** and **8**, whose absorption maxima appear at 579 (55 nm shift) and 590 nm (66 nm shift), respectively. The latter result is noteworthy as the difference between **7** and **8** is the presence of a two-carbon bridge linking each pair of sulfur atoms, thus originating eight-member rings which increase the distortion of the structure (see section 3.4). The absorption redshift, due to the narrowing of the optical band gap, can be attributed to a more destabilized HOMO energy level, a result of the electron donating character of the sulfur atoms [27]. Thus, Table 2 (see section 3.3) shows the electrochemically calculated HOMO and LUMO energies for the studied PDIs. While the LUMO values for PDIs **1**, **2**, **3**, **5**, and **7** remain at a constant value of ca. −3.7 eV, the energies of the HOMOs increase from −6.01 to −5.80, −5.67, −5.69 and −5.58 eV.

Other features observed after the introduction of the S-substituents in the bay positions include 1) the complete loss of the band shape accompanied by a huge widening, and 2) a significant reduction of the molar extinction coefficient, being the largest effects observed again for compound **8**. This second issue is related to a change in the transition dipole moment of the molecules and will be discussed in section 3.4 (*vide infra*).

On the other hand, there are no significant differences between the 1,6 (PDI **3**) and 1,7 (PDI **5**) isomers.

For PDI **10**, substituted at the four ortho positions with alkylthio groups, the shape of the band is slightly preserved, while the redshift is similar to the one produced by one substituent in the bay position (PDI **2**), thus pointing out to the deeper effect caused by substituents in the bay positions than when they are present at the ortho ones. This contrast between the magnitude of the effect caused by the substituents in bay and ortho positions has been previously described [24].

Fig. 2 compares the absorption spectra in dichloromethane solution of the sulfoxide **11** and the sulfone **14** to the one of their precursor, **2**. A hypsochromic shift and a significant shape variation are observed. Thus, PDI **11** shows a band with its maximum located at 524 nm, the same wavelength observed for PDI **1**, together with a shoulder at lower wavelength. On the other hand, PDI **14** has a spectrum which resembles that of the unsubstituted PDI **1** both in wavelength and shape. Interestingly, oxidation of the sulfoxide to the sulfone has almost no influence on the wavelength of the absorption maximum. In fact, it has been previously described that little spectral changes compared with the unsubstituted PDI take place when electron-withdrawing substituents are attached at the bay positions [1b].

Disubstituted PDIs show a similar behavior as monosubstituted PDIs when in dichloromethane solution: sulfoxides and sulfones show a blue shift in the absorption maxima, which lie in the same region as for PDI **1** due to the electron-withdrawing nature of the substituents (*vide supra*). Once again, while the sulfinyl compounds show a band with a shoulder, the spectra of the sulfonyl compounds exhibit the typical vibronic structure of unsubstituted PDIs. Interestingly, PDI **13** (1,7 isomer) presents a higher molar extinction coefficient (ε) than the other derivatives (Fig. 3). We think this is a consequence of a better conjugation pathway in the chromophore due, among other factors, to a less distorted structure of the PDI (see section 3.4).

Comparing tetrasubstituted derivatives in methylene chloride solution, ortho-substituted compounds show higher extinction coeficients than bay-substituted compounds, which could probably be due to the fact that they preserve the planarity of the aromatic core (Fig. S74, ESI). On the other hand, the hypsochromic shift when passing from the sulfide **8** to the sulfone **19** (63 nm) is much higher than the one observed for the couple **7**/**17** (48 nm), being extremely low (6 nm) for the ortho substituted compounds **10**/**18** (Fig. 4).

As a summary, the introduction of electron-donor substituents causes the disappearance of the characteristic vibrational bands of the naked PDI, and a red-shifted broad band can be observed instead. Moreover, the electron donating effect of the alkylthio substituents has a deeper

Table 2
Redox potentials measured by DPV (CH_2Cl_2 solution containing 0.1 M $TBAPF_6$ as the supporting electrolyte and Fc/Fc^+ as the internal standard) and estimated energies of the frontier orbitals.

	$E_{red}2$ (V)	$E_{red}1$ (V)	$E_{ox}1$ (V)	$E_{ox}2$ (V)	LUMO[a] (eV)	HOMO[a] (eV)	Gap (eV)
1	−1.21	−1.1	1.21		−3.7	−6.01	2.31
2	−1.35	−1.13	1	1.38	−3.67	−5.80	2.13
3	−1.42	−1.16	0.87	1.09	−3.64	−5.67	2.03
5	−1.35	−1.13	0.89	1.09	−3.67	−5.69	2.02
7	−1.33	−1.10	0.78	0.90	−3.7	−5.58	1.88
8	−1.19	−0.96	0.84	0.99	−3.84	−5.64	1.8
10	−1.34	−1.14	1.16	1.35	−3.66	−5.96	2.3
11	−1.38	−1.04	1.14	1.3	−3.76	−5.94	2.18
12	−1.47	−0.86	1.33	1.71	−3.94	−6.13	2.19
13	−1.14	−0.86	1.31	1.51	−3.94	−6.11	2.17
14	−1.17	−0.9	1.35		−3.9	−6.15	2.25
15	−1.09	−0.73	1.34		−4.07	−6.14	2.07
16	−1.02	−0.72	1.34		−4.08	−6.14	2.06
17	−0.75	−0.43	1.36		−4.37	−6.16	1.79
18	−0.78	−0.48	1.34		−4.32	−6.14	1.82
19	−0.64	−0.31	1.36		−4.49	−6.16	1.67

[a] Calculated according to the equations: $E_{LUMO} = -E_{red}1 - 4.8$ and $E_{HOMO} = -E_{ox}1 - 4.8$.

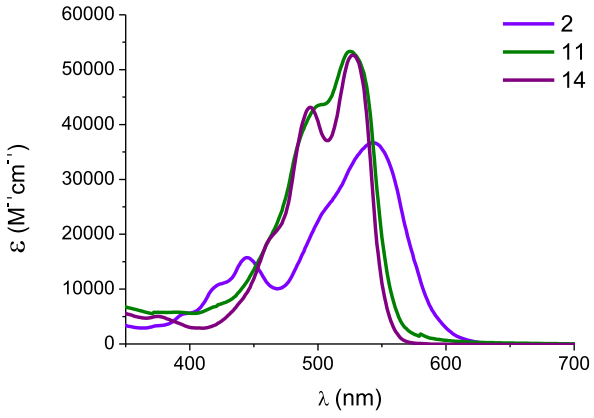

Fig. 2. Absorption spectra of PDIs **2**, **11** and **14** in CH_2Cl_2 solution.

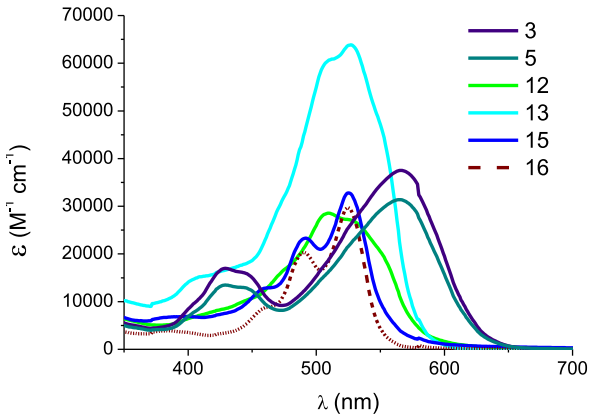

Fig. 3. Absorption spectra of PDIs **3**, **5**, **12**, **13**, **15** and **16** in CH_2Cl_2 solution.

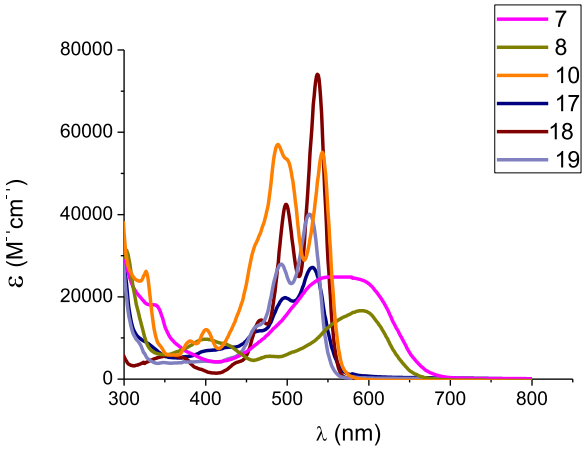

Fig. 4. Absorption spectra of PDIs **7**, **8**, **10**, **17**, **18**, and **19** in CH_2Cl_2 solution.

impact when they are located in the bay positions of the PDI, than when they are located in the ortho ones. On the other hand, replacement of the substituents by electron-acceptor ones leads to the recovery of the vibronic structure in the UV–vis spectra and to a hypsochromic shift of the maxima.

As expected, fluorescence is quenched when donor substituents are introduced, which is attributed to a photoinduced electron transfer process [1b], being more pronounced the effect as the number of groups increases (PDIs **2** to **10**). Thus, the unity quantum yield of PDI **1** drops to 0.049 for PDI **2**, around 0.03 for disubstituted PDIs **3** and **5**, and to 0.001–0.007 for the tetrasubstituted PDIs **7**, **8** and **10**. On the other hand, oxidizing the thioether groups to sulfones leads to a fluorescence quantum yield recovery to values slightly higher than 0.5 for the mono- and disubstituted PDIs, and 0.45 for the bay-tetrasubstituted PDIs, while the ortho-substituted PDI **18** reaches a value of 0.7 (Table 1). Interestingly, oxidation of the thioethers to sulfoxides has no influence on the fluorescence quantum yields. One might be tempted to ascribe the low emission of sulfoxides to the lone pair on the sulfur atom of the sulfinyl group that could undergo a photoinduced electron transfer process, thus quenching the fluorescence. However, it has been proposed that the non-radiative singlet relaxation is due to an excited state pyramidal inversion or to the formation of a twisted intramolecular charge transfer state (TICT) [28].

On the other hand, the existence of appreciable Stokes shifts is principally important for fluorescence practical applications because it allows to separate excitation light from emitted fluorescence using appropriate optics [29]. The fluorescence spectrum of PDI **1** exhibits a small Stokes shift (8 nm, Table 1). The introduction of alkylthio-groups increases the corresponding Stokes shift, from 70 to 80 nm for the mono- and disubstituted PDIs up to 94 nm for PDI **7** with 4 SR groups at the bay positions. This increase of the Stokes shift is dramatically less significant for the *ortho*-tetrasubstituted PDI **10** (14 nm), which is related to the limited impact on the properties caused by the substituents in the ortho positions. On the other hand, sulfinyl derivatives **11**–**13** display Stokes shifts between 40 and 50 nm, while the sulfonyl compounds show values around 15–25 nm.

We have performed a comparative study on the absorption and fluorescence spectra of the family of 1,7-disubstituted PDIs **5** (disulfide), **13** (disulfoxide), and **16** (disulfone) in solvents of different dielectric constant, namely hexane, toluene, dichloromethane, tetrahydrofuran (THF), and acetone (see Figs. S71–S73, ESI). No relation was inferred between the position of the absorption/emission maxima and the solvent dielectric constant for any of the three compounds. The solvatochromic effect was more pronounced for the disulfide (13 nm) and for the sulfoxide (14 nm) than for the sulfone (9 nm). The small solvatochromic effect, especially for the sulfone, points out to an almost absent charge transfer character in the ground state. In contrast, somehow bigger differences could be witnessed in the emission spectra. Thus, in the disulfide there is a difference of 24 nm between the maxima recorded in hexane and dichloromethane, while for the sulfoxide the difference is 28 nm between the maxima in acetone and THF, and for the sulfone is 14 nm between the maxima recorded in hexane and toluene. Finally, for PDI **5** the Stokes shift values lie in the range from 62 to 76 nm, for **13** in the range from 32 to 60 nm, and for **16** the Stokes shifts are almost identical in all solvents (17–22 nm).

3.3. Electrochemistry

Table 2 displays the oxidation and reduction potentials together with the energies estimated for the highest-occupied (HOMO) and lowest-unoccupied (LUMO) molecular orbitals for all derivatives under study. The values indicate a progressive increase of the electron affinity in the series from **11** to **19**.

Fig. 5 compares the redox behavior recorded for compounds **1**, **2**, **3**, **5**, **7**, **8** and **10** using differential pulse voltammetry (DPV). The introduction of an increasing number of thioether groups progressively hinders the reduction process, thus indicating a diminished electron-accepting ability of these compounds compared to **1**. However, bay tetrasubstituted compounds **7** and, especially, **8** are an exception, probably due to their distorted structure, which limits the electron donating influence of the sulfur atoms. On the other hand, the increasing number of thioether groups facilitates the oxidation due to the electron-

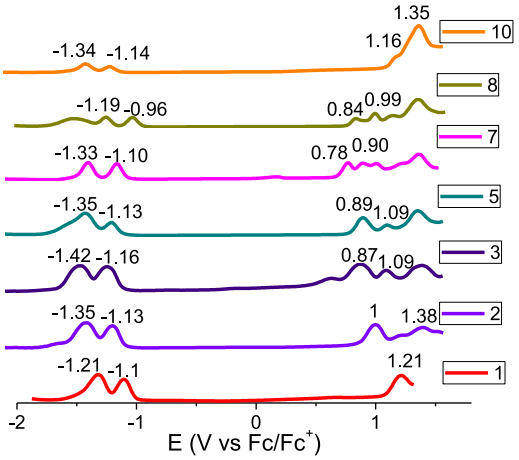

Fig. 5. Differential pulse voltammetry of PDIs **1**, **2**, **3**, **5**, **7**, **8** and **10**.

rich nature of these substituents. The introduction of the substituents at the ortho position (PDI **10**) has a smaller effect in the oxidation potential (1.16 V against Fc/Fc^+) than the bay-substitution (**PDI 7**, 0.78 V against Fc/Fc^+), as commented previously for the optical properties [24].

As expected, oxidation of the sulfur atoms decreases the reduction potential and increases the oxidation one of the compounds. Thus, sulfones **15** and **16** have an increased reduction tendency (−0.73 and −0.72 V, respectively, against Fc/Fc^+) compared to **12** and **13** (−0.862 V against Fc/Fc^+, Fig. 6). No noticeable differences between 1,6 and 1,7 isomers are detected for both the sulfinyl and the sulfonyl compounds.

Tetrasulfones **17**–**19** show an extremely high electron-accepting ability, which is more pronounced for the bay-substituted compounds (Fig. 7). It is remarkable that oxidation of **8** to **19** induces an anodic shift of 650 mV in the reduction potential. The calculated LUMO values for sulfones **17**–**19** are −4.37, −4.32 and −4.49 eV, respectively, which are values very close to the lowest LUMO value described for a PDI (−4.75 eV) [14].

3.4. Theoretical calculations

The energies for the highest-occupied (HOMO) and lowest-unoccupied (LUMO) molecular orbitals, together with the corresponding gaps, were calculated under the density functional theory (DFT) framework (Table 3). Methyl groups were introduced in the imido positions to simplify calculations. The trends observed for the HOMO/LUMO energies and gaps when increasing the number of substituents and its oxidation state agree very well with the experimental data shown in Table 2.

The minimum-energy geometries computed at the B3LYP/6-31G* level of theory for PDIs **8**, **10**, **12**, and **18** are displayed in Fig. 8. The angle formed by the average planes defined by the two naphthaleneimide subunits forming the PDI core (Fig. 8 and Table 3) for PDIs **2**–**8** increases as the number of substituents on the bay area does. Interestingly, for compounds **2**, **3**, **5**, and **11**–**16**, the angles increase in the order sulfoxide < tioether < sulfone. As expected, the most distorted compounds are PDIs **8** and **19**, while the ortho substituted ones, **10** and **18**, are planar or almost planar.

The experimentally observed Stokes shifts point out to consider the need for an optimization of the first excited state, at least for some molecules. Indeed, the calculations performed using the B3LYP functional show a somehow anomalous behavior in some cases. Consequently, we have also used the hybrid meta GGA functional M06-2X, which yields more accurate results for the study of excited states [30].

The optimized structures of the studied compounds in dichloromethane solvation are showed in Figure S74 (ESI). Table 4 shows the vertical and relaxed excitation energies together with their corresponding oscillator strengths calculated from optimized geometries at state-specific solvation (dichloromethane) M06-2X/6-31G* level of theory. The trend of the calculated Stokes shifts matches the experimentally observed one, as shown in Figure S75 (ESI).

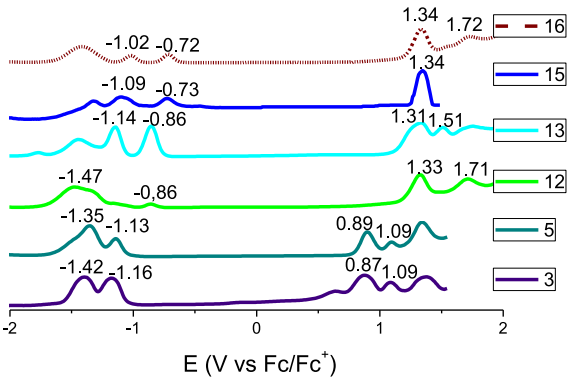

Fig. 6. Differential pulse voltammetry of PDIs **3**, **5**, **12**, **13**, **15** and **16**.

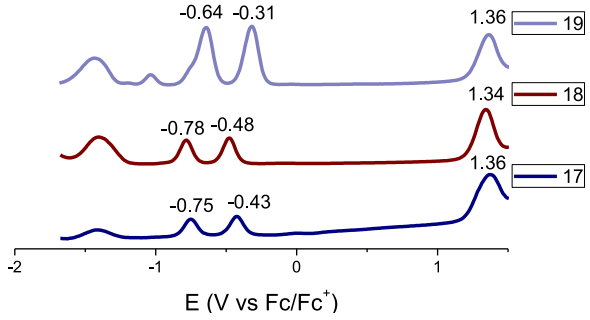

Fig. 7. Differential pulse voltammetry of PDIs **17**, **18** and **19**.

Table 3
Theoretically calculated energies of the frontier orbitals and torsion angles in the bay area for the PDIs in gas phase.

PDI	LUMO (eV)	HOMO (eV)	Gap (eV)	Torsion angle (°)[a]
1	−3.464	−6.000	2.536	0.0
2	−3.443	−5.895	2.452	−17.5/-10.4
3	−3.452	−5.829	2.377	22.4/22.3
5	−3.411	−5.770	2.359	−21.1
7	−3.352	−5.933	2.581	32.6
8	−3.507	−5.882	2.375	−33.7/-35.7
10	−3.289	−5.878	2.589	4.0/4.1
11	−3.606	−6.075	2.469	−15.4/-8.9
12	−3.707	−6.229	2.522	−13/10.9
13	−3.746	−6.150	2.404	−18.7
14	−3.705	−6.271	2.566	−21.1/-11.0
15	−3.797	−6.371	2.580	−24.9
16	−3.814	−6.380	2.566	24.2
17	−4.095	−6.619	2.524	33.8/33.6
18	−4.173	−6.601	2.428	0.3/0.1
19	−4.570	−7.063	2.493	34.2

[a] Angle formed by the average planes defined by the two naphthaleneimide subunits.

Finally, as commented in section 3.2 (*vide supra*), Fig. 1 shows a significant reduction of the molar extinction coefficient of the core-substituted PDIs when compared with PDI **1**. Thus for example, the molar extinction coefficients of PDIs **7**, **8**, and **10**, are between a third and a tenth than the one of PDI **1**. This appears to be not only caused by a change in conjugation due to distortion of the molecular structure, but also a change in the transition dipole moment of the molecules due to the introduction of substituents. Table 5 shows the correlation between the variation in the extinction coefficients and the transition dipole moments for PDIs **1**, **7**, **8**, and **10**.

4. Conclusion

The introduction of thioethers on the PDI core yields electron-donor compounds with oxidation potentials as low as 0.63 V against Fc/Fc^+. On the other hand, oxidation of these compounds renders sulfones with strong electron-accepting character, showing reduction potentials as low as −0.31 V against Fc/Fc^+. Moreover, the functionalization with sulfones of the PDI provides stability by lowering the LUMO to resist ambient oxidation.

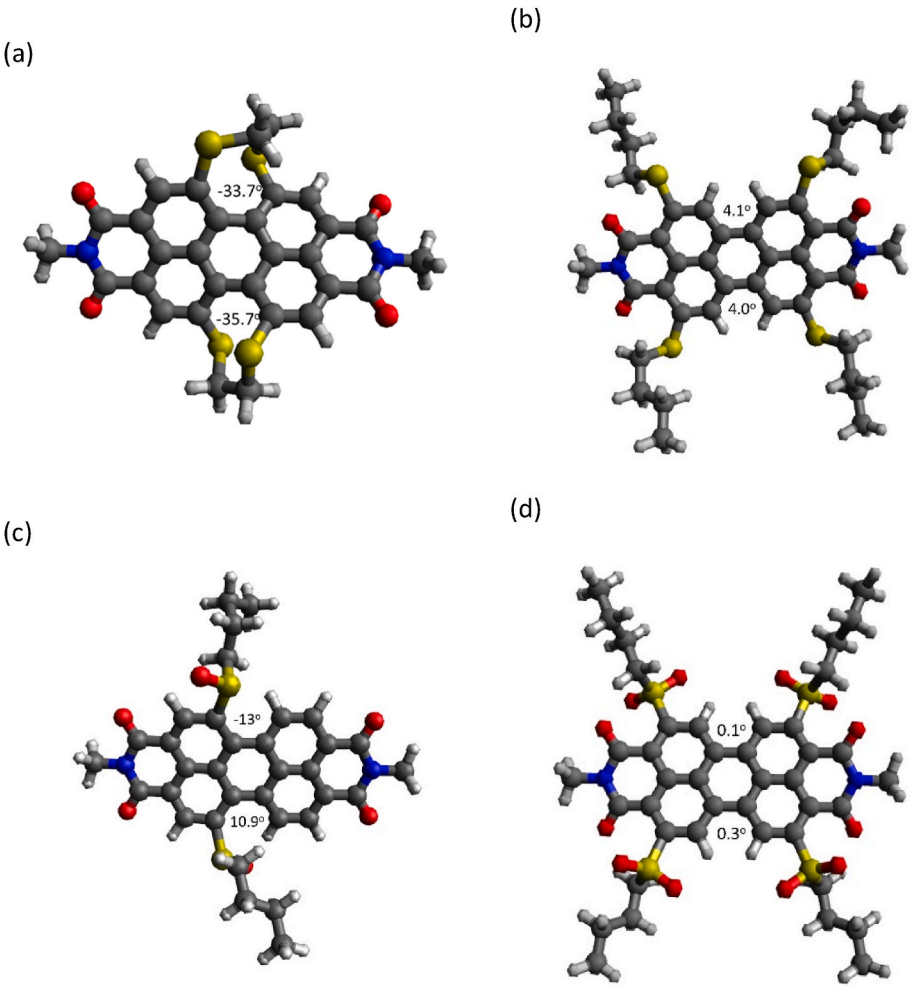

Fig. 8. Torsion angles in the bay region of PDIs **8** (a), **10** (b), **12** (c) and **18** (d).

Table 4
Vertical and relaxed excitation energies (in nm), and oscillator strength (*f*) from optimized geometries at state-specific solvation (dichloromethane) M06-2X/6-31G* level of theory.

PDI	*Vertical Energy (nm)*	*f*	*Relaxed Excitation Energy (nm)*	*f*
1	437	0.799	511	0.777
2	467	0.513	583	0.422
3	482	0.407	618	0.336
5	490	0.418	600	0.391
7	446	0.494	680	0.295
8	498	0.313	662	0.258
10	429	0.702	506	0.731
11	450	0.618	538	0.574
12	441	0.632	563	0.421
13	464	0.503	560	0.470
14	439	0.661	521	0.644
15	443	0.596	524	0.584
16	443	0.586	529	0.577
17	454	0.445	551	0.437
18	460	0.748	542	0.745
19	464	0.447	556	0.454

Table 5
Extinction coefficients (log ε) obtained from the absorption spectra in CH_2Cl_2, and transition dipole moments ($|\vec{\mu}|^2$) obtained from ground to excited state transition electric dipole moments in dichloromethane solvation, for PDIs **1**, **7**, **8**, and **10**.

PDI	log ε	$\|\vec{\mu}\|^2$ (AU)
1	5.2	11.5048
10	4.7	9.9224
7	4.4	7.2526
8	4.2	5.1385

CRediT authorship contribution statement

Nathalie Zink-Lorre: Writing – review & editing, Writing – original draft, Methodology. **Enrique Font-Sanchis:** Formal analysis. **Emilio San-Fabián:** Formal analysis. **Fernando Fernández-Lázaro:** Writing – review & editing, Writing – original draft, Funding acquisition, Conceptualization.

Declaration of competing interest

The authors declare no conflict of interest.

Data availability

No data was used for the research described in the article.

Funding

This research is part of the I+D+i project PID2022-140315NB-I00, funded by MICIU/AEI/10.13039/501100011033 and by ERDF/EU.

Appendix A. Supplementary data

Supplementary data to this article can be found online at https://doi.org/10.1016/j.dyepig.2024.112178.

References

[1] (a) Langhals H. Cyclic carboxylic imide structures as structure elements of high stability. Novel developments in perylene dye chemistry. Heterocycles 1995;40:477–500.(b) Würthner F. Perylene bisimide dyes as versatile building blocks for functional supramolecular architectures. Chem Commun 2004:1564–79.(c) Langhals H. Control of the interactions in multichromophores: novel concepts. Perylene bis-imides as components for larger functional units. Helv Chim Acta 2005;88:1309–43.(d) Würthner F. Bay-substituted perylene bisimides: twisted fluorophores for supramolecular chemistry. Pure Appl Chem 2006;78:2341–9.(e) Hermann A, Müllen K. From industrial colorants to single photon sources and biolabels: the fascination and function of rylene dyes. Chem Lett 2006;35:978–85.

[2] Chesterfield RJ, Mckeen JC, Newman CR, Ewbank PC, da Silva Filho DA, Bredas JL, Miller LL, Mann KR, Frisbie CD. Organic thin film transistors based on N-Alkyl perylene diimides: charge transport kinetics as a function of gate voltage and temperature. J Phys Chem B 2004;108:19281–92.

[3] (a) Huang C, Barlow S, Marder SR. Perylene-3,4,9,10-tetracarboxylic acid diimides: synthesis, physical properties, and use in organic electronics. J Org Chem 2011;76:2386.(b) Li C, Liu MY, Pschirer NG, Baumgarten M, Müllen K. Polyphenylene-based materials for organic photovoltaics. Chem Rev 2010;110:6817–55.(c) Zhan X, Facchetti A, Barlow S, Marks TJ, Ratner MA, Wasielewski MR, Marder SR. Rylene and related diimides for organic electronics. Adv Mater 2011;23:268–84.

[4] Jones BA, Ahrens MJ, Yoon MH, Facchetti A, Marks TJ, Wasielewski MR. High-mobility air-stable n-type semiconductors with processing versatility: dicyanoperylene-3,4:9,10-bis(dicarboximides). Angew Chem, Int Ed 2004;43:6363.

[5] (a) Jung BJ, Tremblay NJ, Yeh ML, Katz HE. Molecular design and synthetic approaches to electron-transporting organic transistor semiconductors. Chem Mater 2010;23:568–82.(b) Anthony JE, Facchetti A, Heeney M, Marder SR, Zhan XW. n-Type organic semiconductors in organic electronics. Adv Mater 2010;22:3876–92.(c) Fan L, Xu Y, Tian H. 1,6-Disubstituted perylene bisimides: concise synthesis and characterization as near-infrared fluorescent dyes. Tetrahedron Lett 2005;46:4443–7.(d) Tan W, Li X, Zhang J, Tian H. A photochromic diarylethene dyad based on perylene diimide. Dyes Pigments 2011;89:260–5.

[6] (a) Wasielewski MR. Self-assembly strategies for integrating light harvesting and charge separation in artificial photosynthetic systems. Acc Chem Res 2009;42:1910–21.(b) Hofmann CC, Lindner SM, Ruppert M, Hirsch A, Haque SA, Thelakkat M, Köhler J. Mutual interplay of light harvesting and triplet sensitizing in a perylene bisimide Antenna−Fullerene dyad. J Phys Chem B 2010;114:9148–56.(c) Blas- Ferrando VM, Ortiz J, Bouissane L, Ohkubo K, Fukuzumi S, Fernández-Lázaro F, Sastre-Santos Á. Rational design of a phthalocyanine–perylenediimide dyad with a long-lived charge-separated state. Chem Commun 2012;48:6241–3.(d) Martín R, Céspedes-Guirao FJ, de Miguel M, Fernández-Lázaro F, García H, Sastre- Santos Á. Single- and multi-walled carbon nanotubes covalently linked to perylenebisimides: synthesis, characterization and photophysical properties. Chem Sci 2012;3:470–5.(e) Flamigni L, Zanelli A, Langhals H, Böck B. Photoinduced processes in a dyad made of a linear and an angular perylene bisimide. Photochem Photobiol Sci 2013;12:2137–45.

[7] (a) Li C, Wonneberger H. Perylene imides for organic photovoltaics: yesterday, today, and tomorrow. Adv Mater 2012;24:613–36.(b) Guide M, Pla S, Sharenko A, Zalar P, Fernández-Lázaro F, Sastre-Santos Á, Nguyen TQ. A structure–property–performance investigation of perylenediimides as electron accepting materials in organic solar cells. Phys Chem Chem Phys 2013;15:18894–9.

[8] (a) Qu J, Kohl C, Pottek M, Müllen K. Ionic perylenetetracarboxdiimides: highly fluorescent and water-soluble dyes for biolabeling. Angew Chem, Int Ed 2004;43:1528–31.(b) Peneva K, Mihov G, Herrmann A, Zarrabi N, Börsch M, Duncan TM, Müllen K. Exploiting the Nitrilotriacetic acid moiety for biolabeling with ultrastable perylene dyes. J Am Chem Soc 2008;130:5398–9.(c) Céspedes-Guirao FJ, Ropero AB, Font-Sanchis E, Nadal A, Fernández- Lázaro F, Sastre-Santos Á. A water-soluble perylenedye functionalised with a 17β-estradiol: a new fluorescent tool for steroid hormones. Chem Commun 2011;47:8307–9.(d) Gálvez N, Kedracka EJ, Carmona F, Céspedes-Guirao FJ, Font-Sanchis E, Fernández- Lázaro F, Sastre-Santos Á, Domínguez-Vera JM. Water soluble fluorescent-magnetic perylenediimide-containing maghemite-nanoparticles for bimodal MRI/OI imaging. J Inorg Biochem 2012;117:205–11.(e) Marcia M, Singh P, Hauke F, Maggini M, Hirsch A. Novel EDTA-ligands containing an integral perylene bisimide (PBI) core as an optical reporter unit. Org Biomol Chem 2014;12:7045–58.

[9] (a) Díaz-García MA, Calzado EM, Villalvilla JM, Boj PG, Quintana JA, Céspedes-Guirao FJ, Fernández-Lázaro F, Sastre-Santos Á. Effect of structural modifications in the laser properties of polymer films doped with perylenebisimide derivatives. Synth Met 2009;159:2293–5.(b) Ramírez MG, Pla S, Boj PG, Villalvilla JM, Quintana JA, Díaz-García MA, Fernández-Lázaro F, Sastre-Santos Á. 1,7-Bay-Substituted perylenediimide derivative with outstanding laser performance. Adv Opt Mater 2013;1:933–8.

[10] (a) Morales-Vidala M, Bojb PG, Quintana JA, Villalvilla JM, Retolazac A, Merinoc S, Díaz-García MA. Distributed feedback lasers based on perylenediimide dyes for label-free refractive index sensing. Sens Actuators B 2015;220:1368–75.(b) Calvo-Gredilla P, García-Calvo J, Cuevas JV, Torroba T, Pablos JL, García FC, García JM, Zink-Lorre N, Font-Sanchis E, Sastre-Santos Á, Fernández-Lázaro F. Solvent-Free off–on detection of the improvised explosive triacetone triperoxide (TATP) with fluorogenic materials. Chem Eur J 2017;23:13973–9.

[11] (a) Gutiérrez-Moreno D, Sastre-Santos Á, Fernández-Lázaro F. Synthesis of bay-triaminosubstituted perylenediimides. Org Chem Front 2018;5:1830–4.(b) Gutiérrez-Moreno D, Sastre-Santos Á, Fernández-Lázaro F. Direct amination and N-heteroarylation of perylenediimides. Org Chem Front 2019;6:2488–99.

[12] (a) Ahrens MJ, Fuller MJ, Wasielewski MR. Cyanated perylene-3,4-dicarboximides and perylene-3,4:9,10-bis(dicarboximide): facile chromophoric oxidants for organic photonics and electronics. Chem Mater 2003;15:2684–6.(b) Jones BA, Facchetti A, Wasielewski MR, Marks TJ. Tuning orbital energetics in arylene diimide semiconductors. Materials design for ambient stability of n-type charge transport. J Am Chem Soc 2007;129:15259–78.

[13] (a) Newman CR, Frisbie CD, da Silva Filho DA, Brédas JL, Ewbank PC, Mann KR. Introduction to organic thin film transistors and design of n-channel organic semiconductors. Chem Mater 2004;16:4436–51.(b) Chang YC, Kuo MY, Chen CP, Lu HF, Chao I. On the air stability of n-channel organic field-effect transistors: a theoretical study of adiabatic electron affinities of organic semiconductors. J Phys Chem C 2010;114:11595–601.(c) Oh JH, Sun YS, Schmidt Rd, Toney MF, Nordlund D, Könemann M, Würthner F, Bao Z. Interplay between energetic and kinetic factors on the ambient stability of n-channel organic transistors based on perylene diimide derivatives. Chem Mater 2009;21:5508–18.(d) Li Y, Tan L, Wang Z, Qian H, Shi Y, Hu W. Inverting the enantioselectivity of a carbonyl reductase via Substrate−Enzyme docking-guided point mutation. Org Lett 2008;10. 529-528.(e) Ahrens MJ, Fuller MJ, Wasielewski MR. Cyanated perylene-3,4-dicarboximides and perylene-3,4:9,10-bis(dicarboximide): facile chromophoric oxidants for organic photonics and electronics. Chem. Mater. 2003;15:2684–6.(f) Gsänger M, Oh JH, Könemann M, Höffken HW, Krause AM, Bao Z, Würthner F. A crystal-engineered hydrogen-bonded octachloroperylene diimide with a twisted core: an n-channel organic semiconductor. Angew Chem, Int Ed 2010;49:740–3.

[14] Zhou Y, Xue B, Wu C, Chen S, Liu H, Jiu T, Li Z, Zhao Y. Sulfur-substituted perylene diimides: efficient tuning of LUMO levels and visible-light absorption via sulfur redox. Chem Commun 2019;55:13570–3.

[15] Zhang Y, Zhou H, Wang X, Li X, Wei J, Qiao Y, Song Y, Gao B. Enhanced brightness and electron affinity of terrylenediimide with sulfone-bridged substituents on the bay región. Chem Commun 2021;57:651–4. See also the correction to this paper: Chem. Comm. 2021;57:813.

[16] Rhys Williams AT, Winfield SA, Miller JN. Relative fluorescence quantum yields using a computer-controlled luminescence spectrometer. Analyst 1983;108:1067–71.

[17] Frisch MJ, Trucks GW, Schlegel HB, Scuseria GE, Robb MA, Cheeseman JR, Scalmani G, Barone V, Petersson GA, Nakatsuji H, Li X, Caricato M, Marenich AV, Bloino J, Janesko BG, Gomperts R, Mennucci B, Hratchian HP, Ortiz JV, Izmaylov AF, Sonnenberg JL, Williams-Young D, Ding F, Lipparini F, Egidi F, Goings J, Peng B, Petrone A, Henderson T, Ranasinghe D, Zakrzewski VG, Gao J, Rega N, Zheng G, Liang W, Hada M, Ehara M, Toyota K, Fukuda R, Hasegawa J, Ishida M, Nakajima T, Honda Y, Kitao O, Nakai H, Vreven T, Throssell K, Montgomery Jr JA, Peralta JE, Ogliaro F, Bearpark MJ, Heyd JJ, Brothers EN, Kudin KN, Staroverov VN, Keith TA, Kobayashi R, Normand J, Raghavachari K, Rendell AP, Burant JC, Iyengar SS, Tomasi J, Cossi M, Millam JM, Klene M, Adamo C, Cammi R, Ochterski JW, Martin RL, Morokuma K, Farkas O, Foresman JB, Fox DJ. Gaussian, Inc., Wallingford CT. 2016.

[18] Becke AD. Density-functional thermochemistry. III. The role of exact exchange. J Chem Phys 1993;98:5648–52.

[19] Francl MM, Pietro WJ, Hehre WJ, Binkley JS, Gordon MS, DeFrees DJ, Pople JA. Self-consistent molecular orbital methods. XXIII. A polarization-type basis set for second-row elements. J Chem Phys 1982;77(7):3654–65.

[20] Hanwell MD, Curtis DE, Lonie DC, Vandermeersch T, Zurek E, Hutchison GR. Avogadro: an advanced semantic chemical editor, visualization, and analysis platform. J Cheminf 2012;4:17.

[21] Zhao Y, Truhlar DG. The M06 suite of density functionals for main group thermochemistry, thermochemical kinetics, noncovalent interactions, excited states, and transition elements: two new functionals and systematic testing of four M06-class functionals and 12 other functionals. Theor Chem Acc 2008;120:215–41.

[22] Yan Q, Zhao D, Conjugated Dimeric, Oligomers Trimeric Perylenediimide. Org Lett 2009;11:3426–9.

[23] Queste M, Cadiou C, Pagoaga B, Giraudet L, Hoffmann N. Synthesis and characterization of 1,7-disubstituted and 1,6,7,12-tetrasubstituted perylenetetracarboxy-3,4:9,10-diimide derivatives. New J Chem 2010;34:2537–45.

[24] Zink-Lorre N, Font-Sanchis E, Sastre-Santos Á, Fernández-Lázaro F. Fluoride-mediated alkoxylation and alkylthio-functionalization of halogenated perylenediimides. Org Chem Front 2017;4:2016–21.

[25] Battagliarin G, Zhao Y, Li C, Müllen K. Efficient tuning of LUMO levels of 2,5,8,11-substituted perylenediimides via copper catalyzed reactions. Org. Letture 2011;13:3399–401.

[26] (a) Zink-Lorre N, Font-Sanchis E, Sastre-Santos Á, Fernández-Lázaro F. Easy and mild fluoride-mediated direct mono- and dialkoxylation of perylenediimides. Dyes Pigments 2016;127:9–17.(b) Zink-Lorre N, Font-Sanchis E, Sastre-Santos Á, Fernández-Lázaro F. Direct alkylthio-functionalization of unsubstituted perylenediimides. Org Biomol Chem 2016;14:9375–83.

[27] Vespa M, Cann JR, Dayneko SV, Melville OA, Hendsbee AD, Zou Y, Lessard BH, Welch GC. Synthesis of a perylene diimide dimer with pyrrolic N–H bonds and N-

functionalized derivatives for organic field-effect transistors and organic solar cells. Eur J Org Chem 2018:4592–9.

[28] (a) Lee W, Jenks WS. Photophysics and photostereomutation of aryl methyl sulfoxides. J Org Chem 2001;66:474–80.(b) Vos BW, Jenks WS. Evidence for a nonradical pathway in the photoracemization of aryl sulfoxides. J Am Chem Soc 2002;124:2544–7.(c) Kathayat RS, Yang L, Sattasathuchana T, Zoppi L, Baldridge KK, Linden A, Finney NS. On the origins of nonradiative excited state relaxation in aryl sulfoxides relevant to fluorescent chemosensing. J Am Chem Soc 2016;138:15889–95.(d) Climent C, Barbatti M, Wolf MO, Bardeen CJ, Casanova D. The photophysics of naphthalene dimers controlled by sulfur bridge oxidation. Chem Sci 2017;8:4941–50.

[29] Sanguineti A, Sassi M, Turrisi R, Ruffo R, Vaccaro G, Meinardia F. High Stokes shift perylene dyes for luminescent solar concentrators. L. Beverina Chem Commun 2013;49:1618–20.

[30] Mahato B, Panda AN. Assessing the performance of DFT functionals for excited-state properties of pyridine-thiophene oligomers. J Phys Chem A 2021;125(1):115–25.